THE CRYSTAL STRUCTURE OF CLAUDETITE (MONOCLINIC As_2O_3)

ALFRED J. FRUEH, JR., *University of Chicago, Chicago, Illinois*

ABSTRACT

From a complete diffraction record of a single crystal of claudetite taken by equi-inclination Weissenburg and Precession techniques, the unit cell dimensions were confirmed as: $a=5.25$ Å, $b=12.87$ Å, $c=4.54$ Å, $\beta=93°49'$. The cell contains four As_2O_3. Due to the apparent faint appearance of an odd order $(0k0)$ reflection, doubt was cast upon the existence of a twofold screw axis (2_1). The presence of the 2_1, and hence of the space group $P2_1/n$, was confirmed by the comparison of the Harker-Patterson sections $P\ (x0z)$ and $P\ (x\frac{1}{2}z)$. From these sections and from Patterson projections on (001) and (100) the eight arsenic atoms were found to be in two general fourfold positions, one set at $x=.258$, $y=.102$, $z=.040$; the other set at $x=.363$, $y=.352$, $z=.007$; and their symmetry equivalents. From electron density projections and intensity checks, the twelve oxygen atoms were found to be in three general fourfold positions at $x=.45$, $y=.22$, $z=.03$; $x=.62$, $y=.41$, $z=.18$; and $x=.95$, $y=.16$, $z=.13$; and their symmetry equivalents. The structure is one of linked AsO_3 groups sharing all oxygens to form an irregular sheet parallel to the perfect (010) cleavage.

INTRODUCTION

Claudetite, the monoclinic form of As_2O_3, is found in nature as a secondary mineral, formed by the oxidation of realgar, arsenopyrite, or other arsenic minerals (1). The habit of its crystals is tabular, forming thin plates on {010}; both penetration and contact twins on {100} are very common. The crystals show perfect micaceous cleavage parallel to {010}. According to Schulman and Schumb (2), claudetite, the high-temperature form, is the stable form of the dimorphous pair, claudetite-arsenolite, at temperatures as low as 2° C. By calculations based upon the measured temperature dependence of the solubilities, these authors conclude that an enantiotropic relation exists between the two forms, the transition temperature being approximately −13° C. The unit cell and space group of claudetite was investigated by Buerger (3) and the following cell dimensions were determined:

$$a=5.25 \text{ Å}$$
$$b=12.87 \text{ Å}$$
$$c=4.54 \text{ Å}$$
$$\beta=93°49'$$

The cell contains four formula weights of As_2O_3. The diffraction symbol is $2/mP2_1/n$, which uniquely fixes the space group as $P2_1/n(C_{2h}^5)$.

EXPERIMENTAL PROCEDURE

The major portion of the data for the present work was obtained from a naturally occurring crystal of claudetite from Jerome, Arizona. Because of the tabular habit, the extreme ease with which these crystals will deform plastically, and the scarcity of untwinned crystals, it was impossible to obtain a crystal of optimum size and shape or to peel a crystal down to a desired shape. Consequently, the crystal used had a *b* axis many times shorter than the other axes. No attempt was made to correct for relative absorption. A complete record of the zero, first, second and third levels of the *c* axis was taken by the equi-inclination Weissenburg method using filtered copper radiation. Zero level *a* and *b* axis records were obtained by the Buerger precession method using filtered molybdenum radiation. Zero level *c* axis data were also obtained by the Weissenburg method from a minute tabular crystal grown from a KOH solution of As_2O_3. Intensity data were gathered from the entire diffraction record in a manner similar to that first suggested by Dawton (4) and adapted to Eastman No-Screen *X*-Ray film by workers in the Massachusetts Institute of Technology crystallographic laboratory (5). The intensities were made proportional to F_{hkl}^2 by correcting for Lorentz and polarization factors as described by Buerger and Klein (6, 7).

CONFIRMATION OF SYMMETRY

Close examination of the zero level *c* axis Weissenburg photographs showed increased blackening along the general radiation streak in the vicinity of (030), which cast doubt on the existence of a true 2_1 axis. To ascertain the existence of this symmetry element and thereby confirm the space group as $P2_1/n$, two Harker-Patterson sections (8), one on $P(x0z)$ and the other on $P(x\frac{1}{2}z)$, were computed by means of Patterson-Tunell strips (9) and are shown in Figs. 1*a* and 1*b*. It is apparent from the larger peaks on the section $P(x\frac{1}{2}z)$, representing a *b* axis translation component of $\frac{1}{2}$, that this translation component must exist in the crystal; hence the twofold screw axis and therefore the space group $P2_1/n$ were

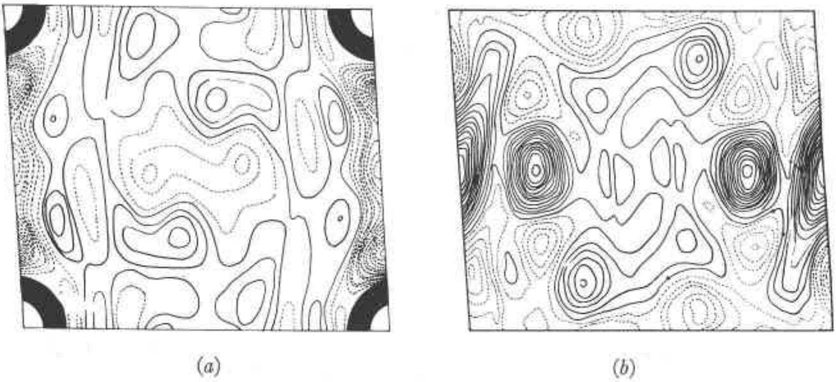
(*a*) (*b*)

FIG. 1. Harker-Patterson sections of claudetite. (*a*) P $(x0z)$. (*b*) P $(x\frac{1}{2}z)$.

confirmed. The high peak about the origin of the $P(x0z)$ would be present regardless of symmetry since it is the zero vector representing each atom to itself.

LOCATION OF THE ARSENIC ATOMS

The arsenic atoms were located from Patterson projections on the (001) and (100) planes illustrated in Figs. 2 and 3 and from the Harker-Patterson section $P(x\frac{1}{2}z)$ mentioned above. In the latter section one elongated peak appeared, due to the presence of two interactions slightly displaced along the axis of elongation. In order to obtain the center of density of each of these interactions and hence the end of the interatomic distance vectors, two graphical sections were made across one of the other peaks known to be a single interaction, and compared at intervals until it was seen that their sum approximated the elongated peak (Fig. 4). The eight arsenic atoms were found to lie in two general fourfold positions, and the following coordinates were determined: As_{I}, $x=.27$, $y=.10$, $z=.03$; As_{II}, $x=.35$, $y=.35$, $z=.00$. The four equivalent points for the

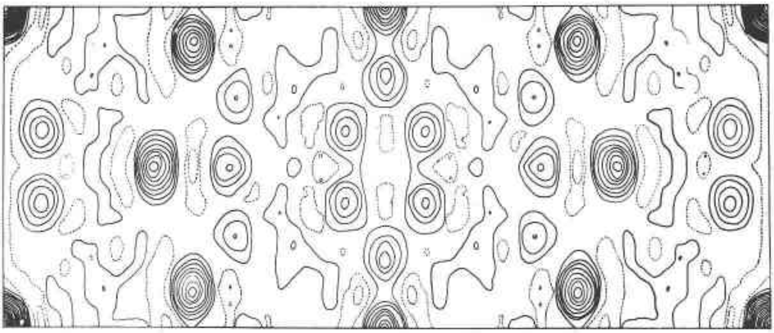

FIG. 2. Patterson projection of claudetite on (001).

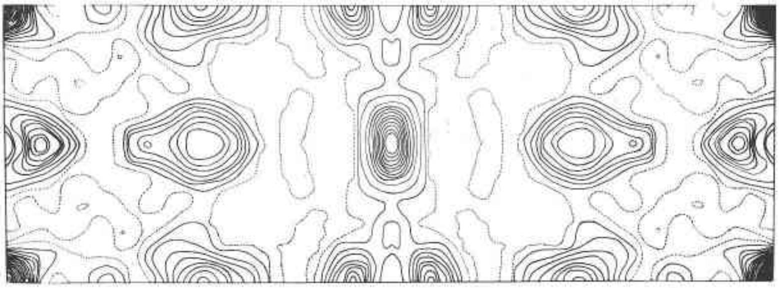

FIG. 3. Patterson projection of claudetite on (100).

general position are: x, y, z; $-x, -y, -z$; $x+\frac{1}{2}, \frac{1}{2}-y, z+\frac{1}{2}$; and $\frac{1}{2}-x, y+\frac{1}{2}, \frac{1}{2}-z$. Not only are all the interactions between arsenic atoms in these locations satisfactorily found on the three vector maps, but also all the sizable peaks on both the Patterson projections can be attributed to interactions between the arsenic atoms. Consequently, it must be assumed that the oxygen-oxygen interactions and the arsenic-oxygen interactions are either masked by arsenic-arsenic interactions or are too comparatively weak to give rise to substantial peaks.

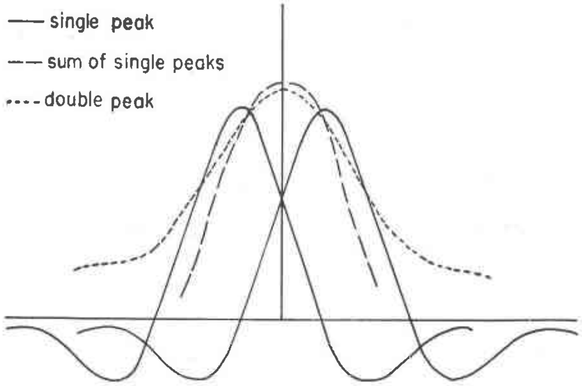

FIG. 4. Graphical sections through single and double Harker-Patterson interaction peaks to determine separation in double peak.

DETERMINATION OF THE OXYGEN PARAMETERS

Electron density projections on (001) and (100) were computed, again by Patterson-Tunell strips, using only those terms whose signs could be unequivocably determined by the arsenic atoms in the locations as found above, the sign determinations being made from the structure factor formula:

$$F_{hkl} = 16 \sum_{n} f_n \cos 2\pi \left(hx + lz + \frac{h+k+l}{4} \right) \cos 2\pi \left(ky - \frac{h+k+l}{4} \right) .$$

The Thomas-Fermi scattering factor for heavy atoms and the Hartree scattering factor for light atoms (10) were used in these calculations. Only about 70% of the available reflections were used in constructing these first electron density projections. These projections yielded one possible general fourfold oxygen location, at $x=.45$, $y=.22$, $z=.03$, and its symmetry equivalent. This location permitted the determination of the signs of additional terms which were in turn employed in making additional electron density projections (Figs. 5*a* and 5*b*). Considerable false detail was present about the arsenic peaks in the projections on the (001) and (100) planes.

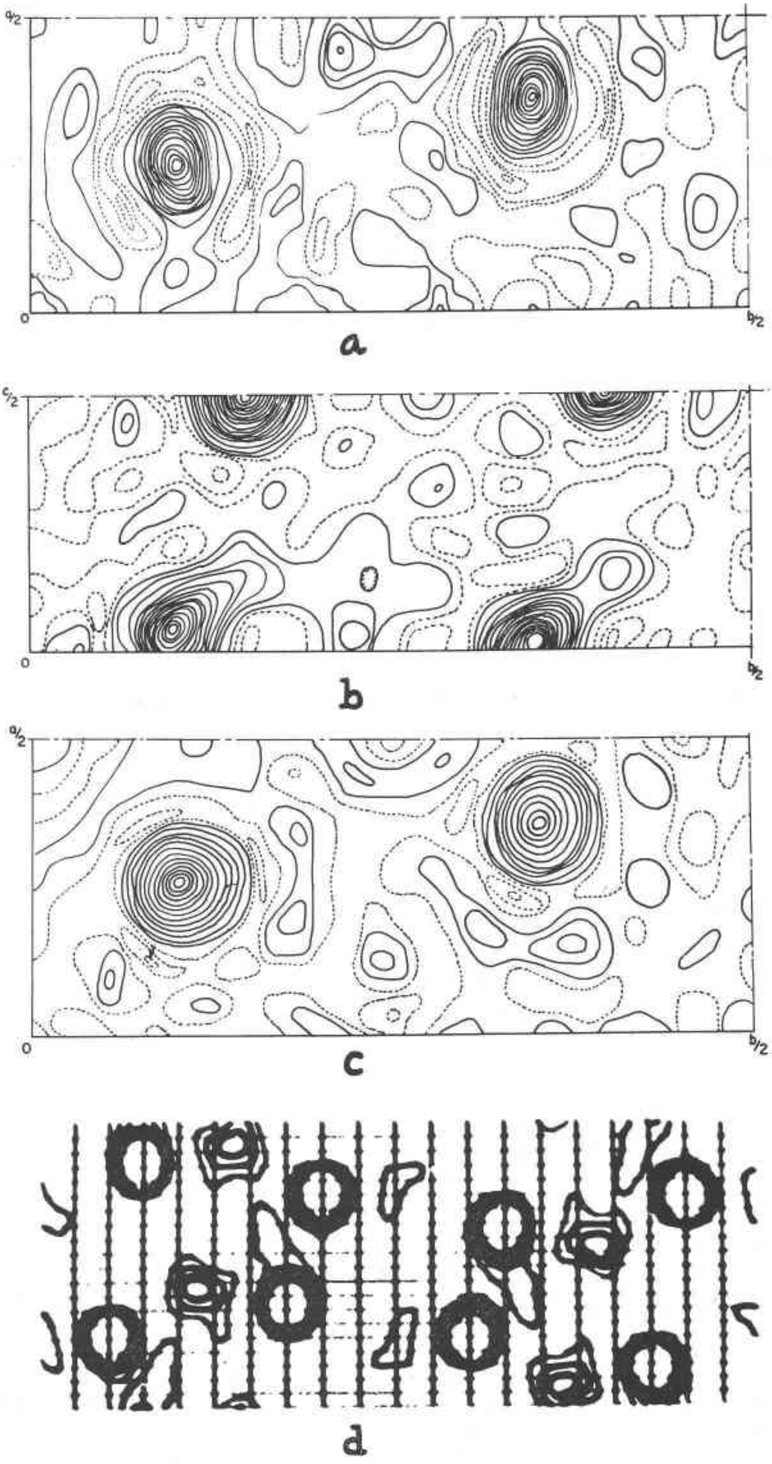

FIG. 5. Electron density projections of claudetite. (*a*) ρ (001) $\frac{1}{4}$ cell. (*b*) ρ (100) $\frac{1}{4}$ cell. (*c*) ρ (001) from calculated arsenic values only. $\frac{1}{4}$ cell. (*d*) ρ (001) from observed values modified by Cesaro Means. Entire cell.

An attempt was made to distinguish between the real oxygen peaks and those peaks due to the false detail about the arsenic atoms. An electron density projection on (001) (Fig. 5*c*) was made using only those terms used in making the same projection as in Fig. 5*a* with F values calculated from the Thomas-Fermi scattering factors of arsenic in the locations determined above. This method was used rather than directly making a difference map (11, 12) expressed by the function:

$$D_{xy} = \rho_0 - \rho_c = \frac{1}{A}\sum_h \sum_k F_0(h0l) - F_c(h0l)e^{2\pi i(hx+ky)}$$

for in the employment of this latter method it would be necessary to determine an atomic form factor, usually expressed in terms of a temperature coefficient, to make the observed values fall off at the same rate as the calculated values. It would also be necessary to scale the F_0 (observed) values with the F_c (calculated) values. By comparing Fig. 5*a* directly with Fig. 5*c* it will be observed that, with the exception of the oxygen peak noted above, most of the peaks on the map made from the observed values are present on the map made from the calculated arsenic values. Therefore, it can be concluded that either the projection of the oxygen peaks coincides with the peaks of arsenic false detail, or the projections of the oxygen peaks are so close to those of the arsenic that they are masked by the arsenic peaks themselves or by the depressions surrounding the peaks. It is also evident that since both maps produced similar amounts of false detail, this false detail can be attributed for the most part to the abrupt termination of the series due to experimental limitations determined by the small cell dimensions in two directions. The application of the temperature factor or absorption corrections would be insufficient to make the Fourier series close.

The series could be made to close falsely by applying the method of the Cesàro means to the coefficients of the series (13). Thus the two-dimensional projection becomes:

$$\rho_{xy} = \frac{1}{A}\sum_h \sum_k F\left(1 - \frac{|h|}{H}\right)\left(1 - \frac{|k|}{K}\right) e^{2\pi i(hx+ky)}$$

where H and K are one greater than the maximum indices h and k used in the series. The results of this series for the (001) projection, as solved by *X-RAC*, are shown in Fig. 5*d*, and it will be noted that the false detail has been removed. Unfortunately, this series exhibits greatly diminished resolving power over the normal series, and any oxygen peaks lying close to arsenics are not resolved. However, the lack of more than one oxygen peak permits the assumption that the other two oxygens lie close to the arsenic in this projection.

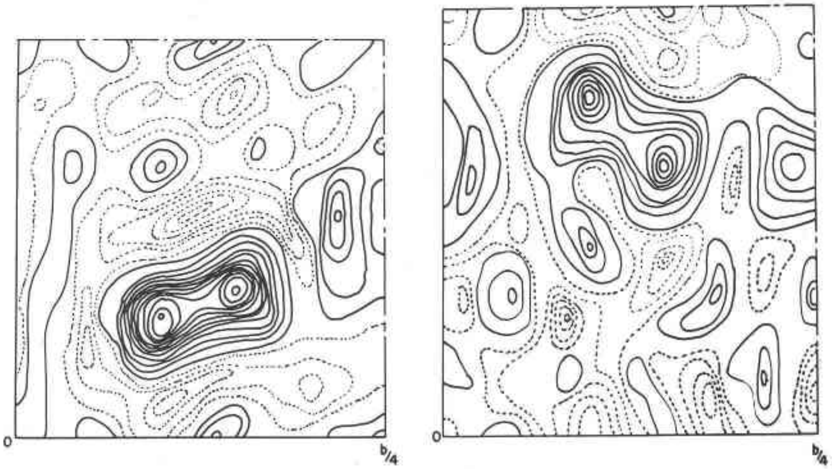

a

b

FIG. 6. Electron density projections of claudetite. (*a*) ρ (101) $\frac{1}{4}$ cell. (*b*) ρ ($\bar{1}01$) $\frac{1}{4}$ cell.

Electron density projections were then made on the (101) and ($\bar{1}01$) planes (Figs. 6*a* and 6*b*), and from these the remaining oxygen parameters were determined to be approximately: $x=.65$, $y=.40$, $z=.14$; and $x=.94$, $y=.14$, $z=.10$. As the contribution of any one oxygen atom has a negligible effect on the signs of the terms of the Fourier series in the electron density projections, the Fourier technique of parameter refining could not be used. Refining was carried out by a system of comparing observed with calculated intensities. The final parameters are listed in Table 1 and in Table 2. The intensities calculated from these parameters are compared with those observed and corrected.

TABLE 1

	x	y	z
$\mathrm{As_{I}}$	.258	.102	.040
$\mathrm{As_{II}}$	.363	.352	.007
$\mathrm{O_{I}}$	.45	.22	.03
$\mathrm{O_{II}}$	.62	.41	.18
$\mathrm{O_{III}}$	.95	.16	.13

Because the scattering power of arsenic is four times that of oxygen at low angles, increasing to over seven times that of oxygen at higher angles, the oxygen parameters can only be determined with limited accuracy.

Table 2*a*. Zero Level *c* Axis. Observed Data from Equi-inclination Weissenburg Record Taken with Copper Kα Radiation and Corrected for Lorentz and Polarization Factors

Index	Sin θ	$\lvert F \rvert$ Calculated	F Observed
0 2 0	.120	4	4
0 4 0	.240	24	17
0 6 0	.360	1	2
0 8 0	.480	8	13
0 10 0	.600	0	0
0 12 0	.719	4	6
0 14 0	.839	0	0
0 16 0	.959	11	18
1 1 0	.159	9	8
1 2 0	.190	4	6
1 3 0	.232	10	8
1 4 0	.281	13	11
1 5 0	.339	3	5
1 6 0	.389	1	2
1 7 0	.445	9	12
1 8 0	.502	19	21
1 9 0	.561	6	7
1 10 0	.617	1	1
1 11 0	.676	2	5
1 12 0	.735	12	23
1 13 0	.794	5	8
1 14 0	.852	1	0
1 15 0	.911	0	0
1 16 0	.971	9	12
2 0 0	.294	10	6
2 1 0	.300	12	12
2 2 0	.317	6	7
2 3 0	.345	1	2
2 4 0	.379	10	12
2 5 0	.420	11	12
2 6 0	.464	7	9
2 7 0	.513	3	4
2 8 0	.563	4	6
2 9 0	.612	8	11
2 10 0	.668	7	11
2 11 0	.722	6	10
2 12 0	.777	1	6
2 13 0	.833	4	6
2 14 0	.889	6	11
2 15 0	.946	6	11

TABLE 2*a* (*Continued*)

Index	Sin θ	$\|F\|$ Calculated	F Observed
3 1 0	.445	4	2
3 2 0	.457	15	16
3 3 0	.476	8	11
3 4 0	.502	3	5
3 5 0	.533	0	0
3 6 0	.569	10	13
3 7 0	.609	6	9
3 8 0	.651	2	4
3 9 0	.695	3	6
3 10 0	.744	0	0
3 11 0	.794	5	6
3 12 0	.844	3	7
3 13 0	.895	6	10
3 14 0	.948	4	7
4 0 0	.588	0	0
4 1 0	.591	0	0
4 2 0	.600	4	7
4 3 0	.616	3	4
4 4 0	.635	1	0
4 5 0	.660	2	5
4 6 0	.689	11	15
4 7 0	.722	1	0
4 8 0	.759	0	0
4 9 0	.796	1	0
4 10 0	.840	13	18
4 11 0	.884	0	2
4 12 0	.929	0	0
4 13 0	.976	1	1
5 1 0	.738	4	3
5 2 0	.744	13	16
5 3 0	.756	4	2
5 4 0	.773	0	1
5 5 0	.794	3	4
5 6 0	.818	8	9
5 7 0	.846	2	0
6 0 0	.882	4	2
6 1 0	.884	1	0
6 2 0	.890	2	1
6 3 0	.900	0	0
6 4 0	.914	3	0
6 5 0	.932	6	6
6 6 0	.952	7	10
6 7 0	.976	4	5

Table 2b. Zero Level *a* Axis. Observed Data from Precession Record Taken with Molybdenum Kα Radiation and Corrected for Lorentz and Polarization Factors

Index	Sin θ	$\lvert F \rvert$ Calculated	F Observed
0 2 0	.055	4	—
0 4 0	.111	24	18
0 6 0	.166	1	2
0 8 0	.221	7	7
0 10 0	.277	0	0
0 12 0	.332	4	0
0 14 0	.387	0	0
0 16 0	.442	11	6
0 1 1	.083	3	4
0 2 1	.096	2	3
0 3 1	.114	5	5
0 4 1	.135	2	0
0 5 1	.159	7	7
0 6 1	.184	0	0
0 7 1	.211	13	10
0 8 1	.235	0	0
0 9 1	.260	13	11
0 10 1	.287	0	0
0 11 1	.314	10	6
0 12 1	.341	1	0
0 13 1	.368	9	5
0 14 1	.393	1	0
0 15 1	.422	9	5
0 0 2	.157	23	18
0 1 2	.159	8	8
0 2 2	.166	3	3
0 3 2	.177	3	6
0 4 2	.192	15	12
0 5 2	.209	2	0
0 6 2	.228	1	0
0 7 2	.249	4	5
0 8 2	.271	7	4
0 9 2	.293	1	0
0 10 2	.319	1	0
0 11 2	.342	1	2
0 12 2	.367	2	1
0 13 2	.393	4	2
0 14 2	.418	1	0
0 15 2	.444	1	0
0 16 2	.469	8	2

TABLE 2*b* (*Continued*)

Index	Sin θ	$\lvert F\rvert$ Calculated	F Observed
0 1 3	.236	0	0
0 2 3	.241	6	6
0 3 3	.249	7	6
0 4 3	.260	3	2
0 5 3	.273	7	6
0 6 3	.288	3	4
0 7 3	.304	12	8
0 8 3	.323	6	4
0 9 3	.341	11	7
0 10 3	.363	0	0
0 11 3	.384	9	6
0 12 3	.407	5	2
0 13 3	.429	8	5
0 14 3	.453	2	0
0 15 3	.477	5	6
0 0 4	.313	12	8
0 1 4	.314	5	3
0 2 4	.318	1	0
0 3 4	.324	5	4
0 4 4	.332	9	5
0 5 4	.342	1	0
0 6 4	.354	1	2
0 7 4	.368	5	5
0 8 4	.384	2	0
0 9 4	.400	4	0
0 10 4	.418	3	0
0 11 4	.437	1	4
0 12 4	.456	0	2
0 13 4	.477	3	2
0 1 5	.393	3	0
0 2 5	.395	5	3
0 3 5	.400	6	5
0 4 5	.407	5	4
0 5 5	.415	3	0
0 6 5	.426	4	0
0 7 5	.437	7	5
0 8 5	.450	9	6
0 9 5	.463	5	5

TABLE 2*c*. SECOND LEVEL *c* AXIS. OBSERVED DATA FROM EQUI-INCLINATION WEISSENBURG RECORD TAKEN WITH COPPER Kα RADIATION AND CORRECTED FOR LORENTZ AND POLARIZATION FACTORS

Index	Sin θ	$\|F\|$ Calculated	F Observed
0 0 2	.340	23	—
0 1 2	.345	8	—
0 2 2	.360	3	2
0 3 2	.384	3	7
0 4 2	.416	15	15
0 5 2	.453	2	2
0 6 2	.495	1	1
0 7 2	.540	5	8
0 8 2	.588	7	8
0 9 2	.636	2	0
0 10 2	.689	2	0
0 11 2	.742	1	3
0 12 2	.796	3	3
0 13 2	.852	4	3
0 14 2	.905	2	0
0 15 2	.961	2	0
1 1 2	.379	2	2
1 2 2	.393	4	3
1 3 2	.415	5	3
1 4 2	.445	7	11
1 5 2	.480	5	6
1 6 2	.519	2	3
1 7 2	.563	10	12
1 8 2	.608	11	19
1 9 2	.655	8	15
1 10 2	.707	0	0
1 11 2	.758	7	8
1 12 2	.812	11	18
1 13 2	.864	6	7
1 14 2	.919	1	0
1 15 2	.974	5	5
$\bar{1}$ 1 2	.370	7	10
$\bar{1}$ 2 2	.385	3	2
$\bar{1}$ 3 2	.412	6	7
$\bar{1}$ 4 2	.437	9	10
$\bar{1}$ 5 2	.473	6	5
$\bar{1}$ 6 2	.513	1	2
$\bar{1}$ 7 2	.557	5	4
$\bar{1}$ 8 2	.603	15	22
$\bar{1}$ 9 2	.649	0	0
$\bar{1}$ 10 2	.702	2	0
$\bar{1}$ 11 2	.754	0	0

TABLE 2c (*Continued*)

Index			Sin θ	$\lvert F\rvert$ Calculated	F Observed
$\bar{1}$	12	2	.807	12	20
$\bar{1}$	13	2	.861	1	1
$\bar{1}$	14	2	.915	1	0
$\bar{1}$	15	2	.971	2	4
2	0	2	.457	8	10
2	1	2	.460	12	12
2	2	2	.472	6	4
2	3	2	.491	9	8
2	4	2	.516	9	12
2	5	2	.546	8	10
2	6	2	.581	6	6
2	7	2	.620	4	3
2	8	2	.663	3	3
2	9	2	.705	4	3
2	10	2	.754	7	7
2	11	2	.802	1	1
2	12	2	.852	1	3
2	13	2	.904	0	2
2	14	2	.955	6	7
$\bar{2}$	0	2	.442	11	17
$\bar{2}$	1	2	.446	10	12
$\bar{2}$	2	2	.458	2	0
$\bar{2}$	3	2	.477	0	0
$\bar{2}$	4	2	.503	10	12
$\bar{2}$	5	2	.534	9	11
$\bar{2}$	6	2	.570	2	3
$\bar{2}$	7	2	.609	5	6
$\bar{2}$	8	2	.652	4	4
$\bar{2}$	9	2	.695	8	12
$\bar{2}$	10	2	.745	4	4
$\bar{2}$	11	2	.794	8	10
$\bar{2}$	12	2	.844	2	0
$\bar{2}$	13	2	.896	5	7
$\bar{2}$	14	2	.949	4	3
$\bar{2}$	15	2	.999	8	15
3	1	2	.518	0	0
3	2	2	.588	12	13
3	3	2	.593	4	5
3	4	2	.614	3	3
3	5	2	.640	6	8
3	6	2	.670	9	8
3	7	2	.704	6	7

TABLE 2c (*Continued*)

Index	Sin θ	$\lvert F \rvert$ Calculated	F Observed
3 8 2	.741	3	4
3 9 2	.780	5	10
3 10 2	.824	1	0
3 11 2	.868	8	10
3 12 2	.915	3	4
3 13 2	.963	7	15
$\bar{3}$ 1 2	.551	7	10
$\bar{3}$ 2 2	.565	14	14
$\bar{3}$ 3 2	.576	10	13
$\bar{3}$ 4 2	.598	2	2
$\bar{3}$ 5 2	.624	2	3
$\bar{3}$ 6 2	.655	9	9
$\bar{3}$ 7 2	.690	8	11
$\bar{3}$ 8 2	.728	2	2
$\bar{3}$ 9 2	.767	2	2
$\bar{3}$ 10 2	.812	0	0
$\bar{3}$ 11 2	.857	4	3
$\bar{3}$ 12 2	.904	4	4
$\bar{3}$ 13 2	.953	5	6
$\bar{3}$ 14 2	.999	4	5
4 0 2	.689	1	1
4 1 2	.691	4	5
4 2 2	.699	4	4
4 3 2	.712	5	7
4 4 2	.729	1	0
4 5 2	.751	3	5
4 6 2	.777	6	6
4 7 2	.807	3	4
4 8 2	.839	1	0
4 9 2	.873	0	0
4 10 2	.913	12	21
$\bar{4}$ 0 2	.669	0	2
$\bar{4}$ 1 2	.672	0	1
$\bar{4}$ 2 2	.680	5	6
$\bar{4}$ 3 2	.693	1	0
$\bar{4}$ 4 2	.711	0	0
$\bar{4}$ 5 2	.733	3	4
$\bar{4}$ 6 2	.754	13	15
$\bar{4}$ 7 2	.790	5	3
$\bar{4}$ 8 2	.823	0	0
$\bar{4}$ 9 2	.858	3	3
$\bar{4}$ 10 2	.898	15	21
$\bar{4}$ 11 2	.939	3	4

TABLE 2c (*Continued*)

Index	Sin θ	$\lvert F \rvert$ Calculated	F Observed
5 1 2	.822	4	4
5 2 2	.828	12	20
5 3 2	.839	4	2
5 4 2	.854	1	0
5 5 2	.872	4	4
5 6 2	.895	7	8
5 7 2	.921	2	0
5 8 2	.950	0	0
5 9 2	.980	3	3
$\bar{5}$ 1 2	.801	0	0
$\bar{5}$ 2 2	.808	15	20
$\bar{5}$ 3 2	.819	2	0
$\bar{5}$ 4 2	.834	0	0
$\bar{5}$ 5 2	.854	2	0
$\bar{5}$ 6 2	.876	9	10
$\bar{5}$ 7 2	.903	3	3
$\bar{5}$ 8 2	.932	2	0
$\bar{5}$ 9 2	.964	4	2
6 0 2	.955	0	0
6 1 2	.957	1	0
6 2 2	.963	2	3
6 3 2	.972	1	2
6 4 2	.985	0	0
$\bar{6}$ 0 2	.934	5	3
$\bar{6}$ 1 2	.936	6	5
$\bar{6}$ 2 2	.942	2	1
$\bar{6}$ 3 2	.952	5	2
$\bar{6}$ 4 2	.965	3	0
$\bar{6}$ 5 2	.981	6	5
$\bar{6}$ 6 2	.999	8	15

DISCUSSION OF THE STRUCTURE

The structure of claudetite can be looked upon as consisting of infinite zigzag chains of

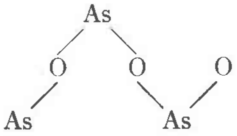

extending in the direction of the *c* axis and being linked together into irregular sheets perpendicular to the *b* axis by additional As-O-As bonds. Thus each arsenic atom is surrounded by three oxygen atoms, and each oxygen has two close arsenic neighbors. The structure is illustrated in Fig. 7.

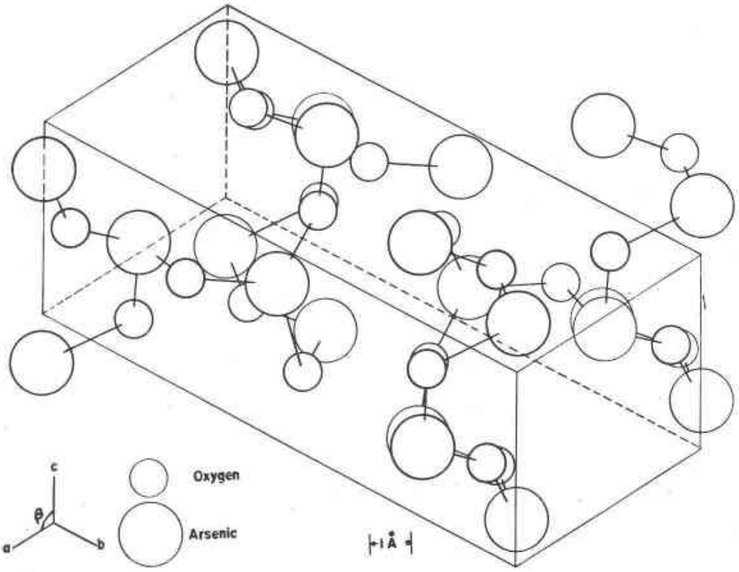

FIG. 7. Crystal structure of claudetite.

Table 3 contains the important interatomic distances.

The As-O distance found in claudetite is the same as the As-O distance of 1.80 ± .02 Å found in the As_4O_6 molecule in the gaseous state and the distance of 1.80 ± .05 Å found in arsenolite (14). Because of the difficulty in obtaining accuracy in the determination of the oxygen parameters, it would be misleading to quote any greater accuracy in the O-O parameters than that given in the table. However, it can be seen that the greater density of claudetite over arsenolite can be accounted for by the closer O-O distances. The closest O-O distance in arsenolite is 2.73 ± .07 Å.

It can be seen that the prominent cleavage and tabular habit of claudetite can be explained by the above structure. The polymorphic relationship between claudetite and arsenolite will be the subject of a future paper.

TABLE 3. SOME IMPORTANT INTERATOMIC DISTANCES IN CLAUDETITE

Atom	Neighbor	Distance
As_I	As_I	3.79
As_{II}	As_{II}	4.07
As_I	As_{II}	3.02
	As_{II}	3.27
	As_{II}	3.30
As_I	O_I	1.82
	O_{II}	1.79
	O_{III}	1.82
As_{II}	O_I	1.77
	O_{II}	1.74
	O_{III}	1.77
O_I	O_{II}	3.0
	O_{II}	2.8
	O_{III}	2.8
	O_{III}	2.4
O_{II}	O_{II}	2.9
	O_{III}	2.8
	O_{III}	2.4

ACKNOWLEDGMENTS

The author is indebted to Professor Martin J. Buerger for his counsel especially during the initial part of the work which was performed in his laboratory in partial fulfillment of the Master's degree at the Massachusetts Institute of Technology. Thanks are also due to Professor R. Pepinsky for suggesting the method of the Cesàro means and for the use of X-RAC. The technical assistance of Anne T. Frueh and W. L. Peterson is gratefully acknowledged.

REFERENCES

1. Palache, C., Berman, H., and Frondel, C., *Dana's System of Mineralogy*, Seventh Edition, 1, 195–197 (1944).
2. Schulman, J., and Schumb, W., The polymorphism of arsenic oxide: *Jour. Am. Chem. Soc.*, **65,** 878–883 (1943).
3. Buerger, M. J., The unit cell and space group of claudetite, As_2O_3: *Am. Mineral.*, **27,** 216 (1942).
4. Dawton, R., The integration of large numbers of *x*-ray crystal reflections: *Proc. Phys. Soc. London*, **50,** 919–925 (1938).
5. Klein, G. E., The crystal structure of nepheline: Master's thesis, Department of Geology, Massachusetts Institute of Technology (1947).
6. Buerger, M. J., and Klein, G., Correction of *x*-ray diffraction intensities for Lorentz and polarization factors: *Jour. App. Phys.*, **16,** 408–418 (1945).
7. Buerger, M. J., and Klein, G., Correction of diffraction amplitudes for Lorentz and polarization factors: *Jour. App. Phys.*, **17,** 285–306 (1946).

8. Harker, D., The application of the three-dimensional Patterson method and the crystal structure of proustite and pyrargyrite: *Jour. Chem. Phys.*, **4**, 381–390 (1936).
9. Patterson, A. L., and Tunell, G., A method for the summation of Fourier series used in the *x*-ray analysis of crystal structures: *Am. Mineral.*, **27**, 655–679 (1942).
10. *Inter. Tabellen z. Best. v. Kristallstrukturen*, Band **II**, 571–572 (1935).
11. Finbak, C., and Norman, N., Subtraction of atom images from a Fourier synthesis of a crystal lattice: *Acta Chem. Scand.*, **2**, 813–827 (1948).
12. Cochran, W., The structure of pyrimidines and purines, Part V: *Acta Cryst.*, **4**, 81–92 (1951).
13. Pepinsky, R., The application of Cesàro means and Parseval's relations in the Fourier analysis of crystals: Abst. *Am. Cryst. Assn.*, Winter meeting, Feb., **1951.**
14. Almin, K. E., and Westgren, A., The lattice parameters of the cubic As_2O_3 and Sb_2O_3: *Arkiv for Kemi, Mineralogie och Geologie*, **15B**, No. 22, 1–6 (1942).

Manuscript received May 28, 1951.